Assessment Of Fundamental Lateral Torsional Buckling As The Minimum Critical Case

Ramy I. Shahin (1),

(1) Higher Institute of Engineering and Technology, Kafrelsheikh, Egypt.
Ramy.Shahin@kfs-hiet.edu.eg, https://orcid.org/0000-0002-4795-8545

Saad A. Yehia (2)

(1) Higher Institute of Engineering and Technology, Kafrelsheikh, Egypt.
saad_yehia@kfs-hiet.edu.eg, https://orcid.org/0000-0002-3069-6059

ABSTRACT

Critical buckling moment is a fundamental property of the flexural resistance of laterally unsupported steel beams. In principle, it is easy to calculate the fundamental critical buckling moment (critical buckling moment for simply supported steel beams with doubly symmetric cross-section subjected to uniform moment). Still, the actual elastic critical moment strongly depends on both the bending moment distribution and restrictions at end supports. Standards estimate the actual critical buckling moment as a multiplier "Moment Gradient Factor" of the fundamental critical buckling moment as what was thought as the most severe case. It is believed that the fundamental critical moment is the minimum critical case for these reasons. First, researchers thought that the fundamental critical moment is the most severe case because studies find that if the moment gradient factor equals one, it tends to be conservative. second, the fundamental critical moment is not more than actual critical moment under a linear moment, distributed load, and concentrated loads. To the authors' knowledge, no study finds cases where the actual critical LTB is less than the critical buckling moment of uniform bending moments due to variation in moment diagram and boundary condition.

This paper studies if the fundamental moment is the minimum critical case by investigating the lateral torsional buckling of twenty representative I-shaped beams subjected to an intermediate moment and two inverted loads with different in-plane and out-of-plane boundary conditions. The actual critical moments are determined numerically using LTBeam and ANSYS, free and commercial software, respectively. The results prove that the fundamental moment is not the minimum critical case under specific loading conditions and show the need to study the cases of critical buckling moments that led to moment gradient factor values of less than one. Further work is required to find cases like this and apply the same loading pattern on single symmetric and cold formed sections to provide a suitable moment gradient factor formula.

Keywords: Elastic Lateral–Torsional Buckling (LTB), Steel beams, Finite ELEMENT Method (FEM), , Steel Standard

Introduction

Structural stability has been a major consideration for as long as steel constructions have existed. The importance of having a good understanding of and implementing the proper member stability checks is growing as computer programs are used more and more in the design of structures. For this reason, it is important to understand the in-plane strength and stiffness response to loadings for steel beams. However, other actions might occur for laterally unrestrained beams when the compression flange is subjected to flexural compression stress (Fig. 1), causing lateral-torsional buckling (abbreviated as LTB) under small loads. In such cases, failure occurs due to instability, and such failure is of elastic nature. The direction of lateral movement is determined by the existing initial imperfection of the unloaded beam.

Consequently, lateral-torsional buckling affects the design of unrestrained beams and beam-column. In the present study, the fundamental critical moment is defined as the critical buckling moment for a simply supported steel beam with a doubly symmetric cross-section subjected to a uniform moment. The fundamental moment causing instability can be obtained using the small deflection theory, as follows [1]:

$$M_{fundamental} = \frac{\pi^2 EI_z}{(kL)^2}\left[\sqrt{\left(\frac{k}{k_w}\right)^2 \frac{I_w}{I_z} + \frac{(kL)^2 GI_t}{\pi^2 EI_z}}\right] \quad (1)$$

This equation calculates the fundamental critical moments for a beam with fork support by setting $\boldsymbol{k} = \boldsymbol{k_w} = 1$. Also, it calculates the fundamental critical moments for beams restrained at ends against lateral bending (weak-axis bending) and warping by modifying $\boldsymbol{k}$ and $\boldsymbol{k_w}$ factors, as shown afterwards. It is worth mentioning that the critical buckling moment for unsymmetrical and single symmetrical sections is out of the scope of this study. For this study, the load is applied on the shear center.

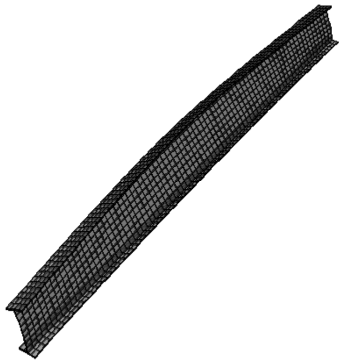

Fig. 1: Lateral Torsional Buckling of a Steel Beam.

In real cases, lateral–torsional buckling is greatly affected by moment, and it was thought that they always provide a higher critical buckling moment. Thus, actual critical LTB can be evaluated using the approximate numerical expressions[2][3] or the Potential Energy Method [4]. However, for practical reasons, consideration of the bending moment diagram is considered by means of the equivalent uniform moment factor, also called the moment gradient correction factor. The fundamental elastic critical moment of the simply supported beam with uniform moment $M_{fundamental}$ is multiplied by this factor to obtain the actual critical LTB for any bending moment diagram. It was thought that this factor is always greater than 1.0 for a varying bending moment diagram [5]. In this section, the critical lateral-torsional buckling moment is proposed by some steel design standards, as follows:

1.1 AISC360-16

The elastic critical lateral-torsional buckling moment is expressed as follows [6][7]:

$$\mathbf{M_{cr} = F_{cr} S_x} \quad (2)$$

Where:

$$\boldsymbol{F_{cr}} = \frac{C_b \pi^2 E}{\left(\frac{L_b}{r_{ts}}\right)^2} \left[\sqrt{\mathbf{1 + 0.078}\ \frac{J_c}{S_x h_o} \left(\frac{L_b}{r_{ts}}\right)^2} \right] \quad \mathbf{(3)}$$

Where L_b is the unbraced lateral displacement or twisting length, S_x is the elastic section modulus about major axe, h_o is the flange centroid distance, and r_{ts} is obtained through the expression:

$$\boldsymbol{r_{ts}} = \left(\frac{\sqrt{I_y C_w}}{S_x}\right)^{\mathbf{0.5}} \quad \mathbf{(4)}$$

This equation is identical to the critical buckling moment expression, included in earlier AISC editions [7], which is expressed by:

$$\boldsymbol{M_{cr} = C_b \frac{\pi}{L_b} \sqrt{E I_y G J + \left(\frac{\pi E}{L_b}\right)^2 I_y C_w}} \quad \mathbf{(5)}$$

The modification factor C_b is used to adjust the critical buckling moment according to the variation in the moment diagram.

1.2 Eurocode 3

This code refers to the European EN-1993-1-1:2005 standard. The capacity of a member subjected to lateral- torsional buckling is reduced by a reduction factor, namely X as shown below[8]:

$$\chi_{LT} = \frac{1}{\phi_{LT} + \sqrt{\phi_{LT}^2 - \bar{\lambda}_{LT}^2}}\ ,\ but\ \ \chi_{LT} \leq 1.0,\ \chi_{LT} \leq \frac{1.0}{\bar{\lambda}_{LT}^2} \quad (6)$$

$$\phi_{LT} = 0.5\left(1 + \alpha_{LT}\left(\bar{\lambda}_{LT} - 0.2\right) + \bar{\lambda}_{LT}^2\right) \quad (7)$$

The slenderness parameter, λ', is inversely proportional to $\sqrt{M_{cr}}$

$$\bar{\lambda}_{LT} = \sqrt{\frac{W_y f_y}{M_{cr}}} \quad (8)$$

The 3-factor formula expression is used to calculate critical moment in early Eurocode editions, but it is not included in the current code. Recently, the formula has been included in Design Guideline ECCS TC 8 [9] and other specifications, such as the Polish Standard [10]. The equation has three correction factors added to the reference case Eq. (1), as follows:

$$M_{cr} = C_1 \frac{\pi^2 E I_Z}{(k_z L)^2} \left[\left(\sqrt{\left(\frac{k_z}{k_w}\right) \frac{I_W}{I_z} + \frac{(k_z L)^2 G I_t}{\pi^2 E I_z} + \left(C_2 z_g\right)^2} \right) - \left(C_2 z_g - C_3 z_j\right) \right] \quad (9)$$

Where C_1 is the moment gradient correction factor, C_2 is the correction factor related to the location of the applied load, and C_3 is the correction factor related to asymmetry about the minor axis. Factor $k_z$is the effective length factor of lateral bending, and factor k_w is the effective length factor of end warping. This equation is equivalent to the AISC expression if C_2 and C_3 are taken equal to zero; the only difference is the notation, and it can be concluded that moment gradient factor C_b and equivalent uniform moment factor C_1 are identical for doubly symmetric members loaded at the shear center.

It is worth mentioning that most studies to estimate C_b focus on linear moment distribution, concentrated load, two concentrated equal loads, concentrated load with one or two end moments, and uniform loading with one or two end moments [1][9]. For all these cases, the actual critical buckling moment M_{cr} is always greater than the fundamental critical moment $M_{fundamental}$. Moreover, it was believed that the uniform moment distribution is the most severe case [5] [18] [16] [19] [20], which suggests that if the moment gradient factor equals one, it tends to be conservative. Since no cases have been previously studied in which the actual critical moments are less than the fundamental moment due to the moment distribution along the beams, the study will move to the methodology used to tackle whether this belief is always true.

2. Numerical Modeling of Lateral Torsional Buckling

So far, Finite Element [14] and Finite Difference techniques remain the best choices to study the lateral-torsional buckling phenomenon. Two different programs (i.e., LTBeam and ANSYS) are utilized in this study to solve the LTB problem. A brief explanation for their application to estimate M_{cr} is presented as follows.

2.1 LTBeam

This study uses a finite element-based program (LTBeam) to calculate the critical buckling moment of beams by modelling beams as shell elements and solving the classic eigenvalue problem using an iterative process. The program is based on the Vlasov thin-walled beam theory, which assumes that the section does not distort in its plane and that shear deformations are negligible. Under these assumptions, it is well-established that the critical moment for the fundamental case is the lowest possible. The program was developed in collaboration between CTICM and the European Community for Steel and Coal. Users can download and install the program for free. The program is recommended in previous studies [1], [13][16] [20], and validated with other FEM programs and references [17].

2.2 ANSYS

It is possible to perform lateral torsional buckling analysis using ANSYS software through eigenvalue analysis, also known as buckling analysis. Since ANSYS is generic finite element software, the boundary conditions are not pre-defined as in LTBeam software, so it is required to implement loads and boundary conditions in the finite element model.

Fork support is implemented as illustrated in Fig. 1 (a), (b), and (c). For beams restrained against lateral bending and warping, remote displacement boundary conditions are implemented, as illustrated in Fig. 1 (d), to force the slave nodes to move with the master node for the coupled degrees-of-freedom specified by the user.

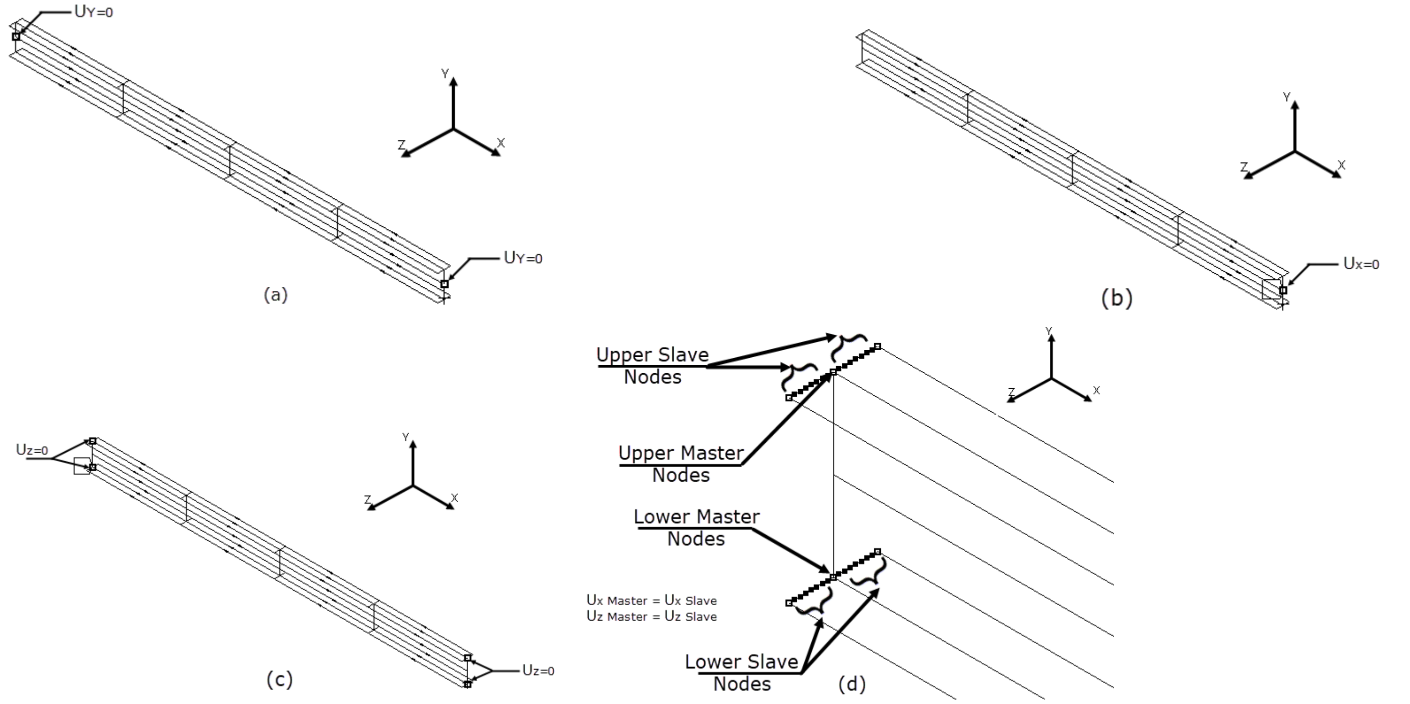

Fig. 2: Restrained Boundary Conditions (a) Vertical Displacement (b) Longitudinal Displacement (c) Torque and Lateral Displacement (d) Lateral Bending and Warping

Finite elements (SHELL 181) are used for modelling flange and web elements, and beam elements (BEAM 189) are used at support and loads locations to avoid any artificial localized effects under point loads/moments/reactions that will not take place in actual construction details (which inevitably distribute all "point" loads on some area of the cross-section), this element is added at web and having cross-section equal to web thickness.

2.3 Validation

The study validates (LTBeam) and ANSYS FEM with the fundamental critical moment $M_{fundamental}$ for the cases studied in the next section so that they will be mentioned there. Currently, the study verifies the moment gradient factor calculated by (LTBeam) and ANSYS FEM with the potential energy formulas developed by Trahair [3], results obtained from the potential energy method by Yoo et al.[4], and well-known moment factors [1] for the following load cases Fig. 3 :

1. Concentrated load and one end moment.

2. Linear moment distribution.
3. Uniformly distributed load and one end moment.

The moment gradient factor is calculated using the finite element method in the following way: The fundamental critical moment $M_{fundamental}$ is calculated using equation (10), and M_{cr} is calculated using LTBeam and ANSYS programs. Hence, equation (9) can be expressed as:

$$M_{cr} = C_1 \ M_{fundamental} = C_1 \frac{\pi}{k_z L} \sqrt{E \ I_y G \ J + \frac{1}{k_z k_w} \left(\frac{\pi \ E}{L}\right)^2 I_y C_w} \qquad (11)$$

Since the actual critical moment M_{cr} and the fundamental $M_{fundamental}$ are known, the moment gradient factor is determined using the expression:

$$C_b = \ C_1 = \frac{M_{cr}}{M_{fundamental}} \qquad (12)$$

2.4 Comparison and Discussion

Fig. 4, Fig. 5, and **Error! Reference source not found.** show that the results obtained from (LTBeam) and ANSYS are close to the potential energy formulas. However, in most cases, it is noted that when attempting to model the given problems using a shell element in (ANSYS) program, the results are a few per cent lower than that based on a thin-walled beam element in (LTBeam) program. The reason is attributed to cross-sectional distortion, which is captured in shell analysis but omitted in thin-walled beam analysis based on the Vlasov theory. For this reason, the critical $M_{Fundamental}$ estimated from shell finite element analysis (ANSYS) is employed in the study besides theoretical$M_{Fundamental}$.

On the other hand, (LTBeam) and ANSYS results conform with the results obtained from the potential energy method by Yoo et al.[4] and well-known moment factors [1] as shown in **Error! Reference source not found.** It is worth mentioning that the Yoo and Lee factor regarding the beam subjected to a concentrated load at mid-span is similar to Trahair equation for the first case with end moments equal to zero. However, there is a slight difference between the findings (1.35 from Trahair equation and 1.36 from Yoo and Lee), while (LTBeam) and ANSYS results reached 1.36.

The general conclusion drawn from the above-mentioned comparative analysis is that there is good accordance between the moment gradient factor determined by the potential energy method, well-known formulas, and FEM results. Furthermore, the reliability of LTBeam and ANSYS seems quite reasonable.

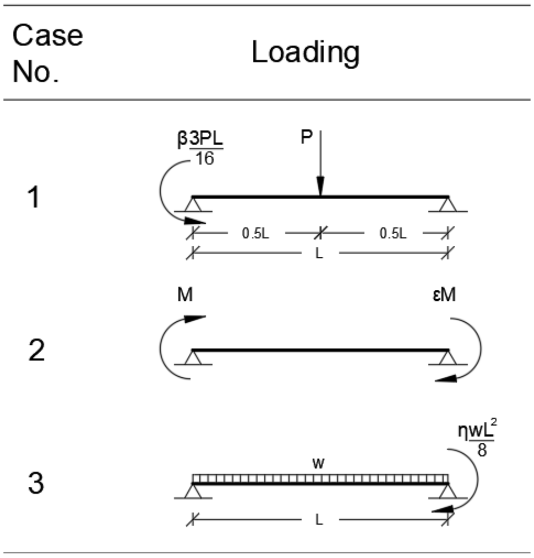

Fig. 3: Verification load Cases.

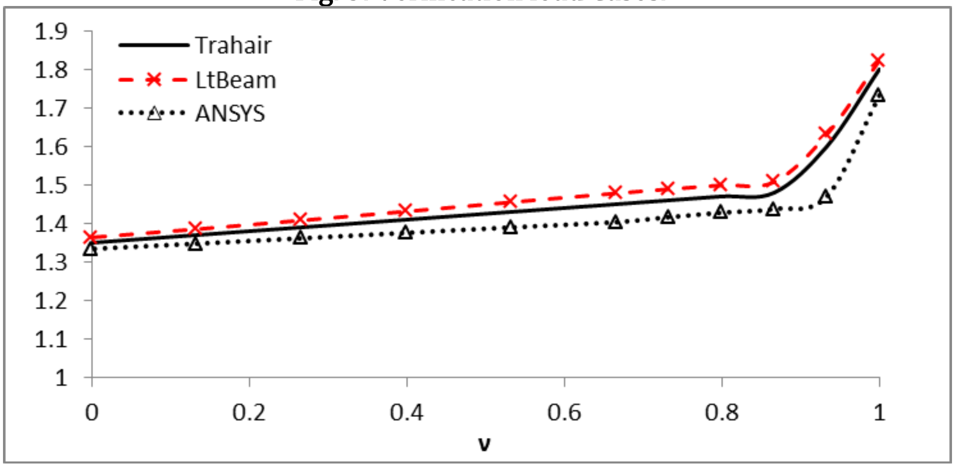

Fig. 4: Moment Factor Verification for Case (1).

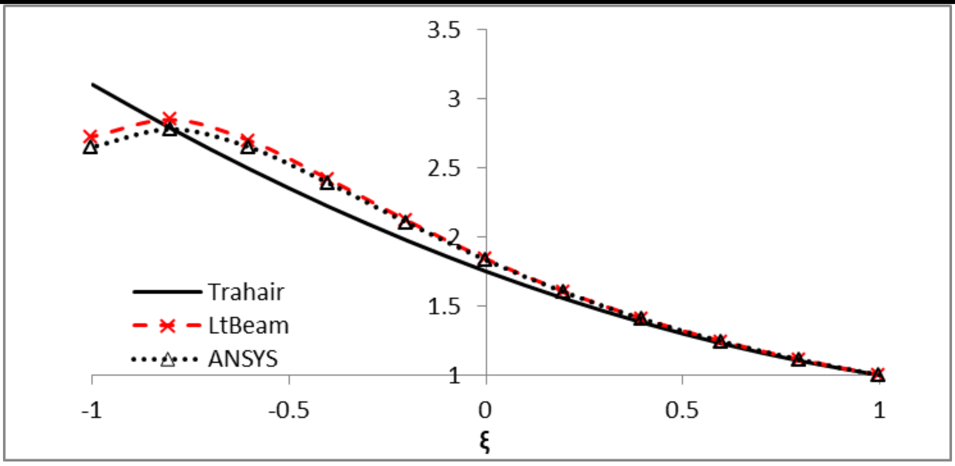

Fig. 5: Moment Factor Verification for Case (2).

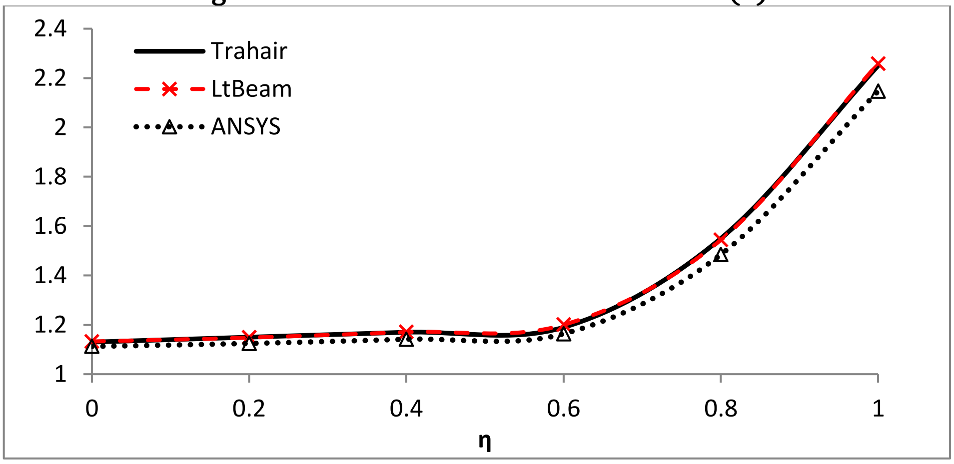

Fig. 6: Moment Factor Verification for Case (3).

Table 1: Verify LTBeam and ANSYS Results with Yoo et al. Method &Well-Known Moment Gradient Factors

Loading	Support Conditions	Yoo& Lee	NCCI	FEM LTBeam	FEM ANSYS
Uniform bending		1	1	1	1
Uniformly distributed load		1.13	1.127	1.13	1.134
		-	2.578	2.61	2.423
Concentrated load at mid-span		1.36	1.348	1.363	1.364
		-	1.683	1.725	1.671
Concentrated loads at the third points		1.04	-	1.09	

3. Case Study

The study investigates the critical buckling moment for beams subjected to intermediate moment and two reversed loads through the following steps (Fig. 7):

1- Calculate the $M_{fundamental}$ “critical buckling moment for simply supported steel beams with doubly symmetric cross-section subjected to uniform moment” for a beam with specific length, cross-section, and different lateral bending and warping end conditions;

2- Calculate the actual critical LTB M_{cr} for the beam mentioned above under an intermediate moment and two reversed loads with different end conditions.
3- Track cases where the M_{cr} is less than $M_{fundamental}$

Four steel sections are employed in this study.

(1) The first section is a built-up section with the same depth, width, flange thickness, and web thicknesses as (IPE300) profile without radius at flange-to-web junction. Following are the section properties of the simplified IPE300 section: $I_z = 602.71\ cm^4$, $I_t = 15.222\ cm^4$, $I_w = 126108\ cm^6$, and the span of the beam is 5000 mm.

(2) The second section is a built-up section with the same depth, width, flange thickness, and web thicknesses as (HEA300) profile without radius at flange-to-web junction. Following are the section properties of the simplified HEA300 section: $I_z = 6301.3\ cm^4$, $I_t = 59.085\ cm^4$, $I_w = 1.200E + 06\ cm^6$, and the span of the beam is 10000 mm.

(3) The third section is a built-up section with the same depth, width, flange thickness, and web thicknesses as (HEB240) profile without radius at flange-to-web junction. Following are the section properties of the simplified HEB240 section: $I_z = 3918.5\ cm^4$, $I_t = 82.871\ cm^4$, $I_w = 487160\ cm^6$, and the span of the beam is 10000 mm.

(4) The fourth section is a built-up section with a total depth of 300 mm, web thickness of 8 mm, flange width of 150 mm, and flange thickness of 8 mm. This section is designed to have a buckling length bigger than the elastic critical (LTB) as discussed below. Following are the section properties of the I300×8-150×8 section: $I_z = 3918.5\ cm^4$, $I_t = 82.871\ cm^4$, $I_w = 487160\ cm^6$, and the span of the beam is 5000 mm.

Material properties for steel sections are E= 200000 Mpa, υ= 0.3, G= 76923 Mpa, steel grade is A36.

All sections satisfy these conditions:

(A) The beams are restrained at ends only,

(B) Steel sections are subjected to (LTB) since the buckling length L_b exceeds the unrestrained critical length corresponding to the plastic bending moment L_p, where L_p is expressed in ANSI/AISC 360-16 as:

$$L_p = 1.76\ i_y \sqrt{E/f_y} \quad (13)$$

(C) Flange local buckling and compression flange yielding will not occur since the steel sections have compact flanges and webs, as defined in ANSI/AISC 360-16.

(D) The slenderness ratio of the minor axe is less than 200. See Table 2.

It is worth mentioning that there is another critical unrestrained length L_r which is the length when elastic lateral–torsional buckling occurs

$$L_r = 1.95\ r_{ts} \frac{E}{0.7\ f_y} \sqrt{\frac{I_t}{S_x\ h_0}} \sqrt{1 + \sqrt{1 + 6.76 \left(\frac{0.7\ f_y}{E} \times \frac{S_x\ h_0}{I_t}\right)^2}} \quad (14)$$

Consequently, it is important to compare critical unrestrained lengths "$L_p, and\ L_p$" with the buckling length of beams. The buckling length L_b is more than the critical unbraced length for the limit state of yielding L_p for all sections, but the buckling length L_b is less than the elastic critical buckling length L_r for simplified IPE300, HEA300, and HEB200 sections. For this reason, the fourth section I300×8-150×8 is employed here, where the buckling length is more than L_r. It can be concluded from Table 2 that cases $L_p < L_b \leq L_r$ and $L_b > L_r$ are employed in the study. It is also concluded that the nominal flexural strength M_n is governed by the (LTB) M_{cr} because $\frac{M_{cr}}{M_p}$ is less than one, where M_p is the Nominal flexural strength due to plastic bending moment as per AISC360-16 specifications.

Table 2 L_r, L_p, M_{cr}, M_P for sections

Beam	L_b (m)	L_p (m)	L_r (m)	L_b/L_p	L_b/L_r	M_p (kN.m)	M_{cr} (kN.m)	M_{cr}/M_p	λ_y

IPE300	5	1.7	5.36	294.1%	93.3%	149.44	98.2	65.7%	146.7
HEA300	10	3.85	13.2	259.7%	75.8%	323.92	247.06	76.3%	129.86
HEB200	10	2.58	13.09	387.6%	76.4%	153.89	112.88	73.4%	193.99
I300x10-150x8	5	1.55	4.86	322.6%	102.9%	127.01	73.75	58.1%	160.89

3.1 Calculating the Theoretical Fundamental Critical (LTB) Moment $M_{fundamental}$

The 3-factor formula expression is used to calculate the theoretical fundamental critical moment $M_{fundamental}$ by setting the moment gradient factor to equal $C_1 = 1$; setting correction factors to equal zero:$C_2 = C_3 = 0.0$. Consequently, data sets are collected for double symmetric sections loaded at the shear center.

Factors k_z and k_w are similar to the buckling length factor for a compression member and are equal to 1.0 unless a special provision for lateral bending and warping fixity is made. However, where lateral bending and warping are restrained, these factors are calculated as follows: $k_z = k_w = \sqrt{k_1 k_2}$, where $k_1$and k_2 refer to lateral bending and warping coefficients at the left and right ends, respectively. Factors $k_1$and k_2 equal 1.0 when lateral bending and warping are permitted, and they equal 0.5 when lateral bending and warping fixity is made [11]. Accordingly, there are three cases where lateral bending and warping are well defined:

1- The common case of normal support conditions at the ends (fork supports), k_z and k_w are equal to 1.
2- The case where lateral bending and warping are fixed at one end and free at the other. For example, if the lateral bending and warping are fixed at the left support ($k_1 = 0.5$) and free at the right ($k_2 = 1.0$), then$k_z = k_w = \sqrt{k_1 k_2} = 0.707$.
3- The case where lateral bending and warping are fixed at both ends, $k_z$and $k_w$are equal to 0.5.

The study verifies the theoretical $M_{fundamental}$ using the 3-factor formula with LTBeam and ANSYS programs, and the difference between results is computed:

$$\Delta_{LTBeam} = \frac{|M_{fundamental}(Theoritical) - M_{fundamental}(LTBeam)|}{M_{fundamental}(Theoritical)}$$

$$\Delta_{ANSYS} = \frac{|M_{fundamental}(Theoritical) - M_{fundamental}(ANSYS)|}{M_{fundamental}(Theoritical)}$$

Table 3 show a good agreement between outputs. It is also noticed that ANSYS outputs tend to be a few smaller than theoretical $M_{fundamental}$ in most cases, which will be explained in the next section.

Table 3 Verify the 3-factor formula with ANSYS and LTBeam

Section	Lateral Support	$M_{fundamental}$ 3 Moment Eq.	LTBeam	ANSYS	Δ_{LTBeam}	Δ_{ANSYS}
IPE300	Fork Support	101.86	101.53	101.04	0.32%	0.80%
	Fixed - Free	174.01	176.71	175.44	1.55%	0.82%
	Fixed - Fixed	314.13	313.21	309.98	0.29%	1.32%
HEA300	Fork Support	294.24	293.25	285.69	0.34%	2.91%
	Fixed - Free	482.15	488.82	477.63	1.38%	0.94%
	Fixed - Fixed	837.98	835.19	819.29	0.33%	2.23%
HEB200	Fork Support	126.10	125.66	123.12	0.35%	2.37%
	Fixed - Free	185.71	187.51	184.41	0.97%	0.70%
	Fixed - Fixed	282.36	281.39	279.98	0.34%	0.84%
I300x8-150x8	Fork Support	73.97	73.76	74.56	0.28%	0.79%
	Fixed - Free	127.97	130.06	130.15	1.63%	1.70%
	Fixed - Fixed	233.43	232.85	230.18	0.25%	1.39%

3.2 Estimating Actual Critical Buckling (LTB) moment M_{cr} for a Beam Loaded by Intermediate Moment and two Reversed Loads.

3.2.1 Loading Conditions (Fig. 7):

This paper studies five load cases. These cases are different in terms of distribution of bending diagram, end moments, and restrained lateral bending and warping at beam ends as follows (Fig. 7):

A. The first condition consists of a beam resting on fork supports, so the lateral bending and warping at the ends are free($k_1 = k_2 = 1$).
B. The second condition is like case A, except that the lateral bending and warping are fixed on the left end($k_1 = 0.5, k_2 = 1$).
C. The third condition is like case B, except for an end moment at the left. ($k_1 = 0.5, k_2 = 1$)
D. The fourth condition is like case C, except that the lateral bending and warping at the ends are fixed ($k_1 = k_2 = 0.5$).
E. The fifth condition is like case A, except that the lateral bending and warping are free at the left and fixed at the right ($k_1 = 1, k_2 = 0.5$).

The end moments are the fixed end moments for rigid-pinned members, as shown in (Fig. 8), and $M_{fundamental}$ calculated above is mentioned briefly for each case in Fig. 7.

No.	Case of Loading	$k = \sqrt{k_1 k_2}$	Corresponding Fundamental "Uniform Moment" Case	$M_{fundamental}$ (kN.m) IPE300	HEA300	HEB200	I300x8-150x8
A	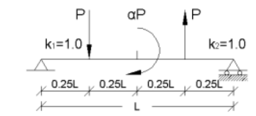	1.00		101.86	294.24	126.10	73.97
B	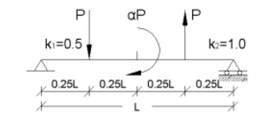	0.707	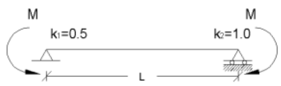	174.01	482.15	185.71	127.97
C	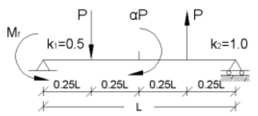	0.707		174.01	482.15	185.71	127.97
D	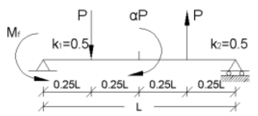	0.50		314.13	837.98	282.36	233.43
E	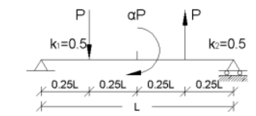	0.50		314.13	837.98	282.36	233.43

Fig. 7: Load Cases.

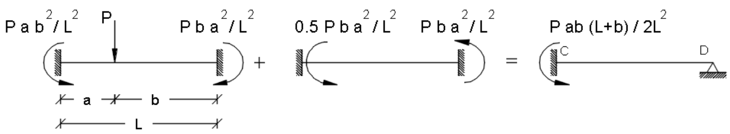

(A) Concentrated Force.

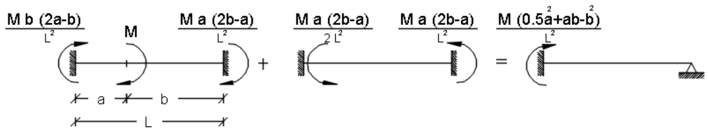

(B) Intermediate Moment.

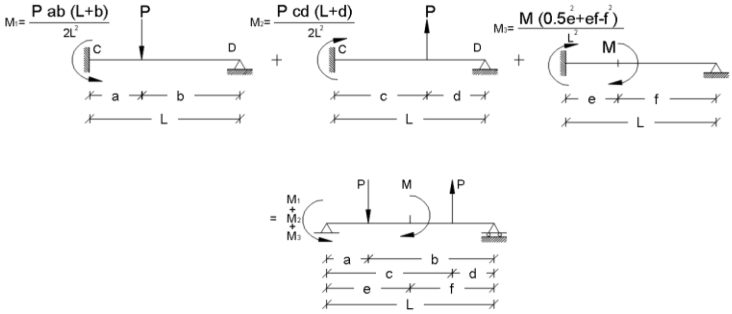

(C) Intermediate Moment and Two Reversed Forces.

Fig. 8: Fixed End Moment for Rigid-Pinned Members.

3.3 Discussion

It is noteworthy to observe the change in the moment gradient factor in response to the distribution of the bending diagram. Let us start from case A. Fig. 9 shows that critical M_{cr} is approaching the fundamental $M_{fundamental}$, while α ratio "α is indicated in Fig. 7" is approaching 0.83, 1.67, 1.66, and 0.83 for IPE300, HEA300, HEA200, and I300x8-150x8 respectively. However, M_{cr} is still not less than $M_{fundamental}$.

The results from case A show that the moment critical moment is not below the fundamental buckling moment. Thus, this excludes the possibility of a detrimental effect due to distortion greater than the beneficial effect of the moment gradient, which results in a critical buckling moment less than the fundamental critical moment.

Moving on to other cases: the results of B, C, D, and E are unique as Fig. 10, to Fig. 13 show situations where M_{cr} is less than $M_{fundamental}$. Even though there is a small dispersion between $M_{fundamental}$ results collected from LTBeam, ANSYS, and the 3-factor formula for cases B, C, D, and E, as discussed before, this deviation does not affect the final conclusion, because the actual critical buckling moment M_{cr} is lower than fundamental $M_{Fundamental}$ with significant ratios as shown in these figures. Particularly, it is consistently found in Table 4 that the actual moments M_{cr} are lower than the fundamental $M_{fundamental}$ in most cases and could go down by 29% in some cases.

Table 4: Ratio between Critical and Fundamental LTB Moment

Beam		*IPE300*				*HEA300*				*HEB200*				*I300x8-150x8*			
Case		B	C	D	E	B	C	D	E	B	C	D	E	B	C	D	E
$\frac{M_{Critical}}{M_{Fundamental}}$	LTBeam	0.80	0.90	0.84	1.02	0.80	0.88	0.85	0.73	0.78	0.86	0.83	0.73	0.80	0.90	0.84	0.75
	ANSYS	0.81	0.91	0.83	1.02	0.78	0.86	0.82	0.71	0.76	0.84	0.81	0.71	0.83	0.93	0.85	0.75

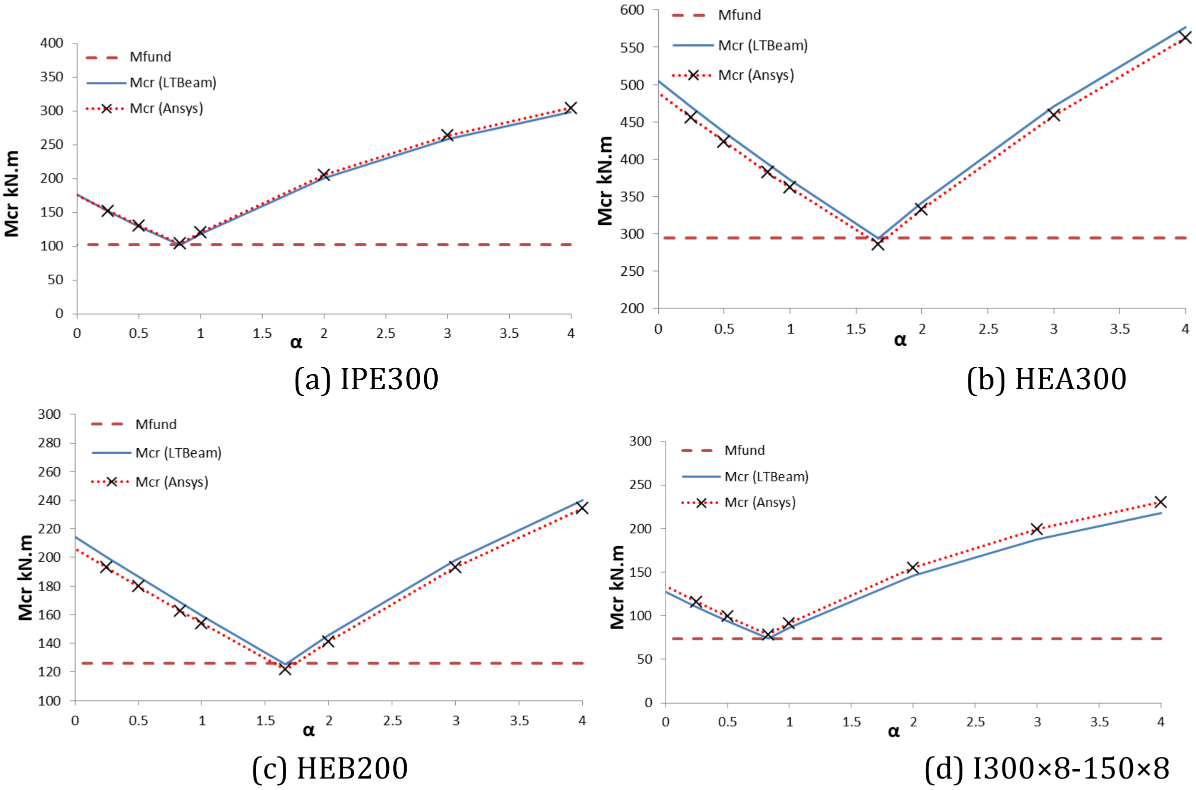

(a) IPE300 (b) HEA300

(c) HEB200 (d) I300×8-150×8

Fig. 9: Critical and Fundamental Buckling Moment for Case A.

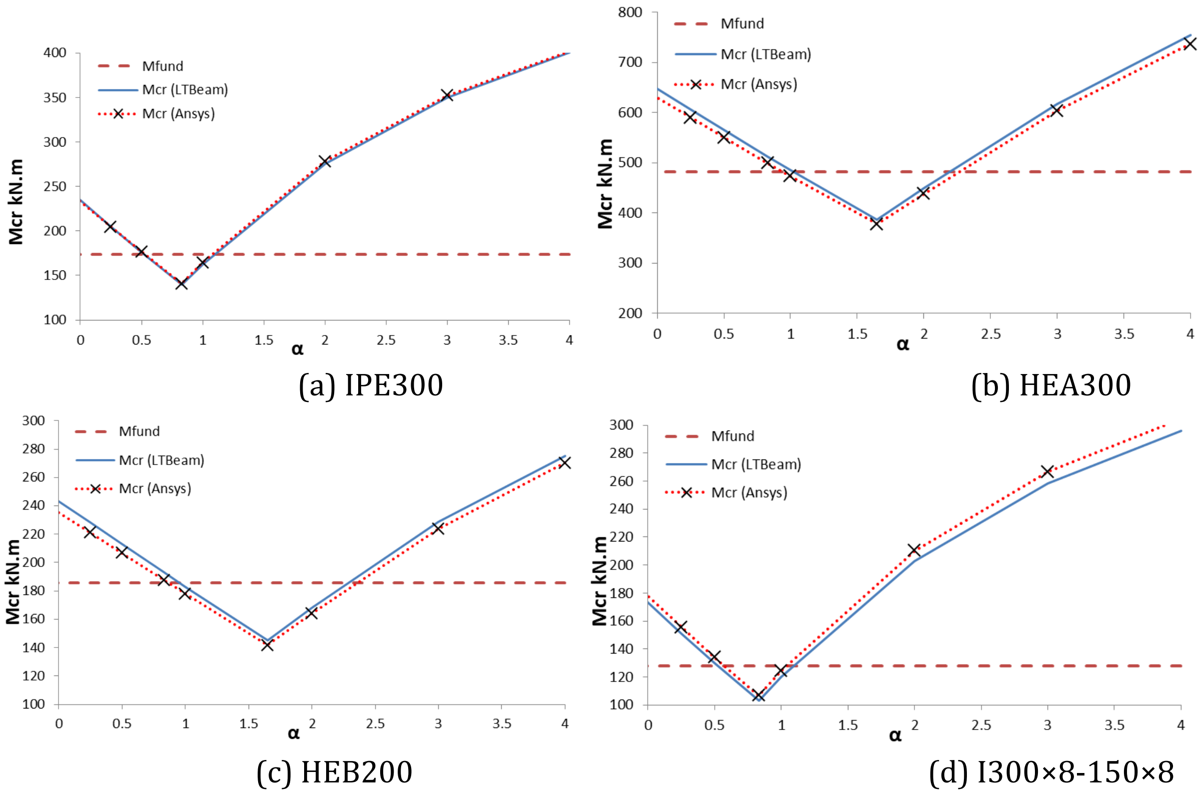

(a) IPE300 (b) HEA300

(c) HEB200 (d) I300×8-150×8

Fig. 10: Critical and Fundamental Buckling Moment for Case B.

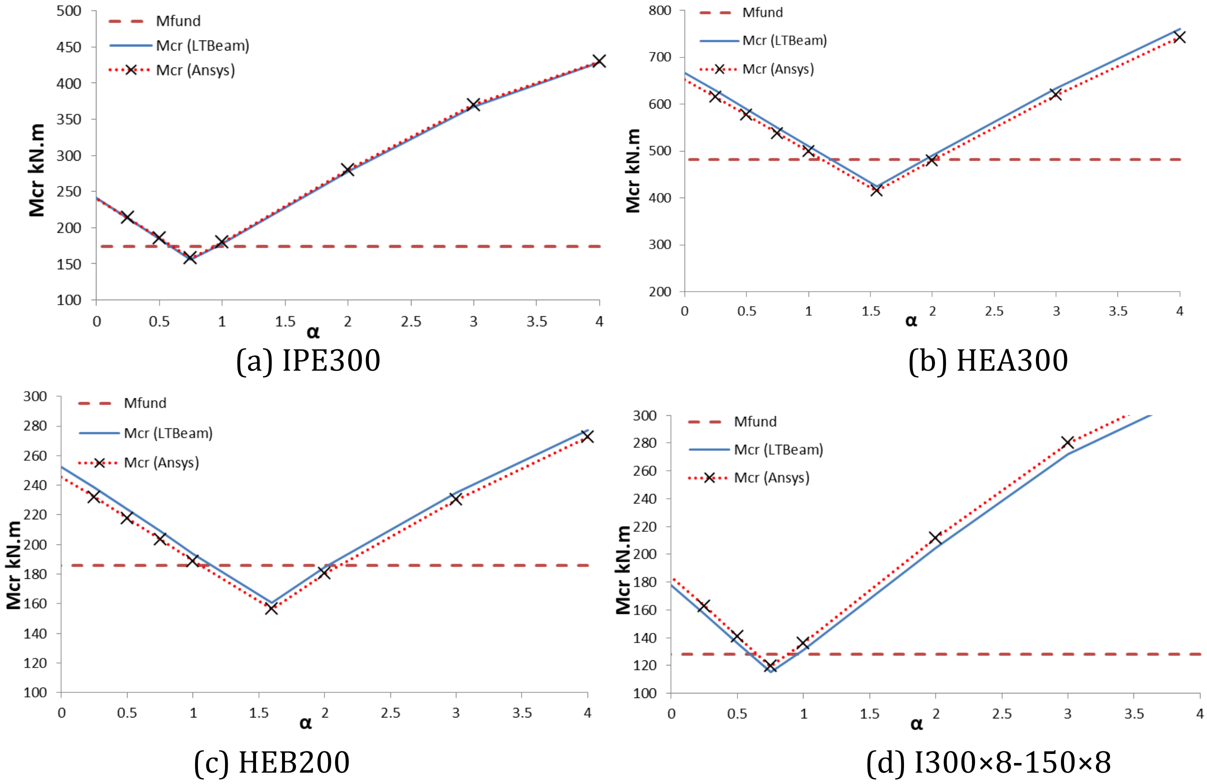

(a) IPE300 (b) HEA300

(c) HEB200 (d) I300×8-150×8

Fig. 11: Critical and Fundamental Buckling Moment for Case C.

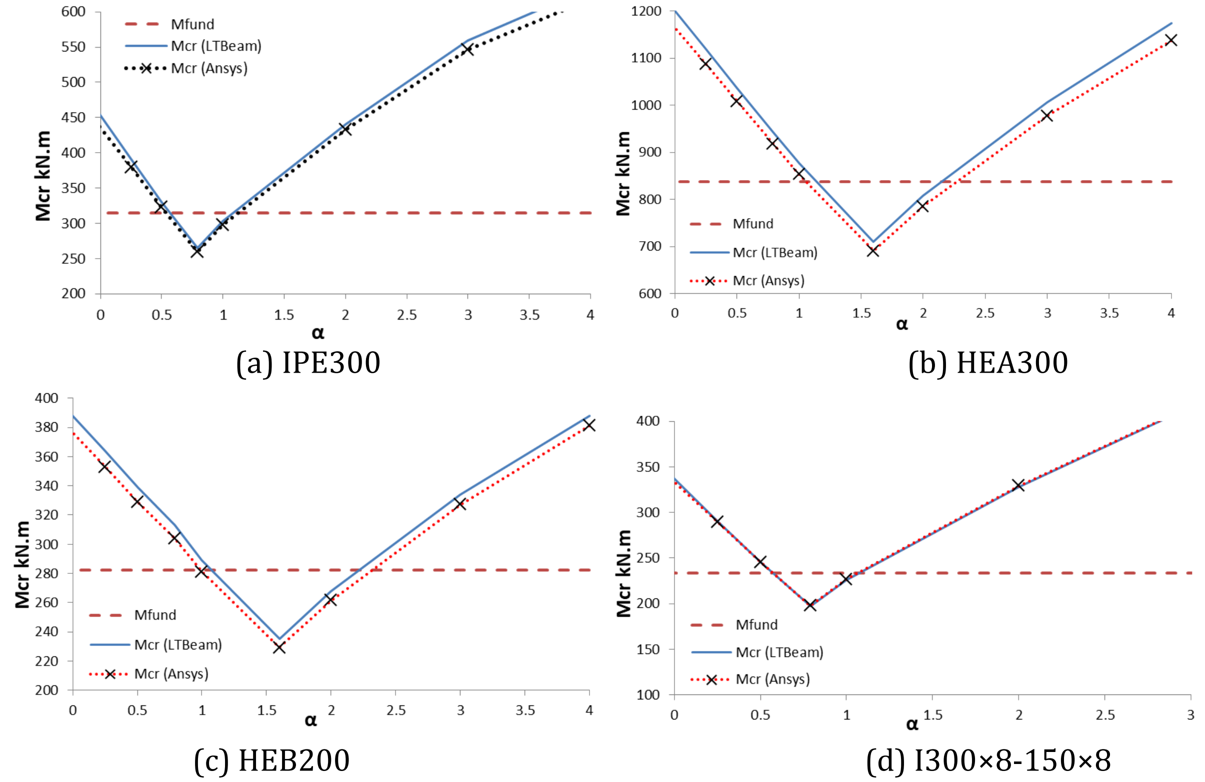

(a) IPE300 (b) HEA300

(c) HEB200 (d) I300×8-150×8

Fig. 12: Critical and Fundamental Buckling Moment for Case D.

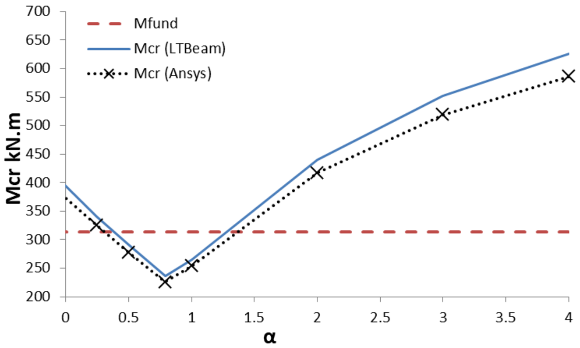

(a) IPE300

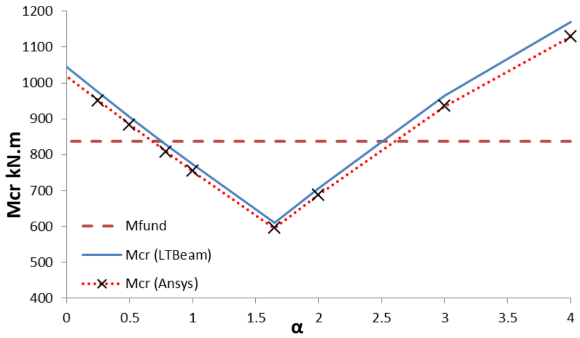

(b) HEA300

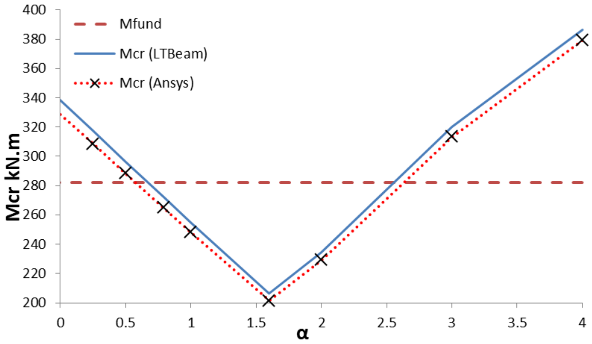

(c) HEB200

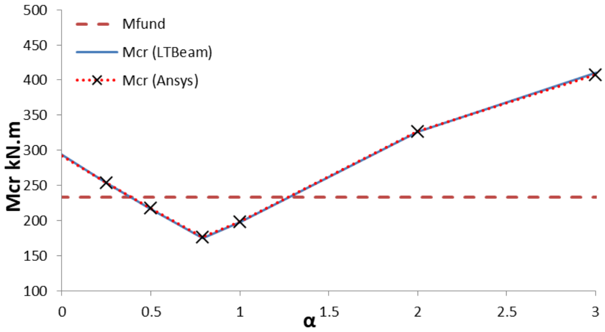

(d) I300×8-150×8

Fig. 13: Critical and Fundamental Buckling Moment for Case E.

This discovered phenomenon is significant for the following reasons:

1- It was believed that the critical moment using a uniform moment diagram is the most severe case [5] [18] [16] [19] [20].In addition, current critical (LTB) moment equations in AISC360-16 (and other similar design standards such as CAN/CSA-S16-14, AS-4100 (1998), etc.) prescribe a moment gradient factor of 1.0 for T-shaped beams [20]. The author believes that further studies for T shapes sections would imply that the actual critical (LTB) could be less than the fundamental critical moment.

2- For the expressions developed in the U.S. standards, Moments M_A, M_B, M_C in Eq. (10) and Eq. (11) can't be more than M_{max}, so the minimum moment gradient factor is 1.

3- To the authors' knowledge, the reasons for reducing the critical (LTB) for the double symmetric I section are related to material-specific phenomena like imperfection, residual stresses, and load height to the centroid. So, for double symmetric sections loaded at the centroid, the moment modification factor is always greater than 1.0 for a varying bending moment diagram [5]. However, in some cases, further reductions in critical moment predictions may occur in shell finite element models due to localized buckling/deformation that may take place under the application of point loads, point moments, or reactions. It is thus important to verify this is not the case by examining the buckling mode shapes and taking precautions in the modeling to avoid any artificial localized effects under point loads/moments/reactions that will not take place in actual construction details (which inevitably distribute all "point" loads on some area of the cross-section). In this study, precautions are taken by adding beam elements at supports and loads locations at quarter points, as discussed earlier, see Fig. 14 and Fig. 15. These figures also show the eigenvalue buckling does not show local buckling modes.

4- No single study finds cases where the value of critical LTB is less than the fundamental critical moment due to variation in the moment diagram and boundary conditions.

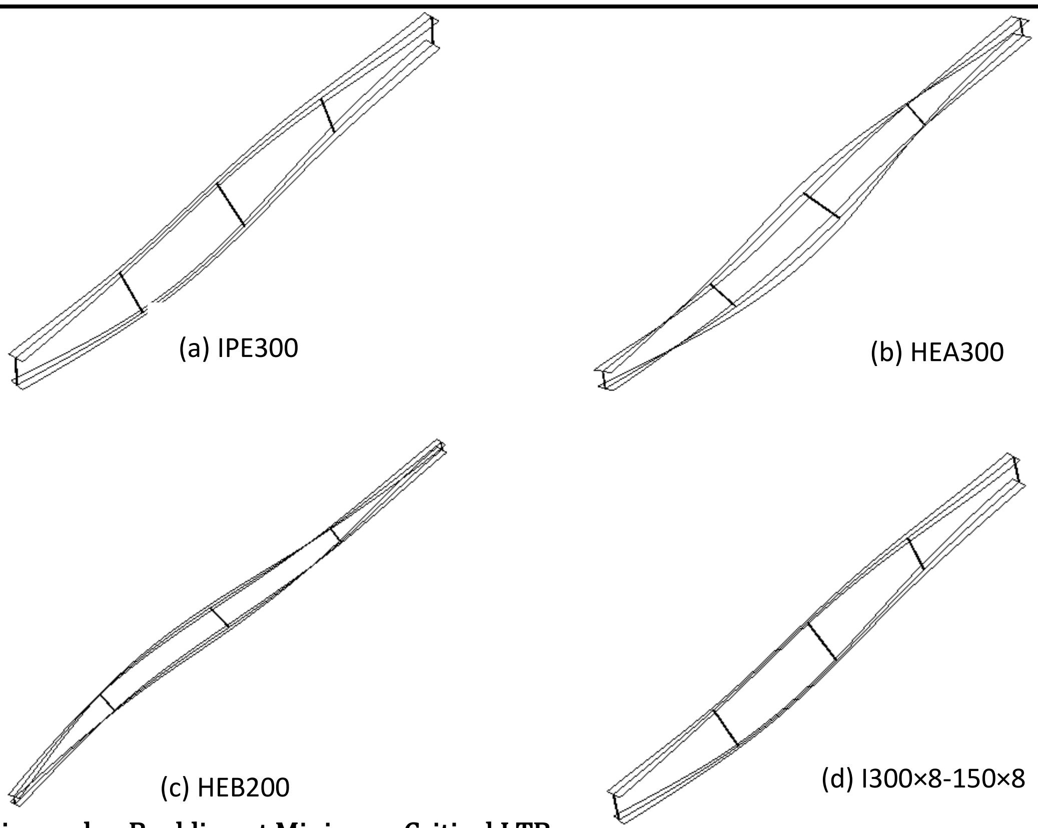

Fig. 14: Eigenvalue Buckling at Minimum Critical LTB (Case B)

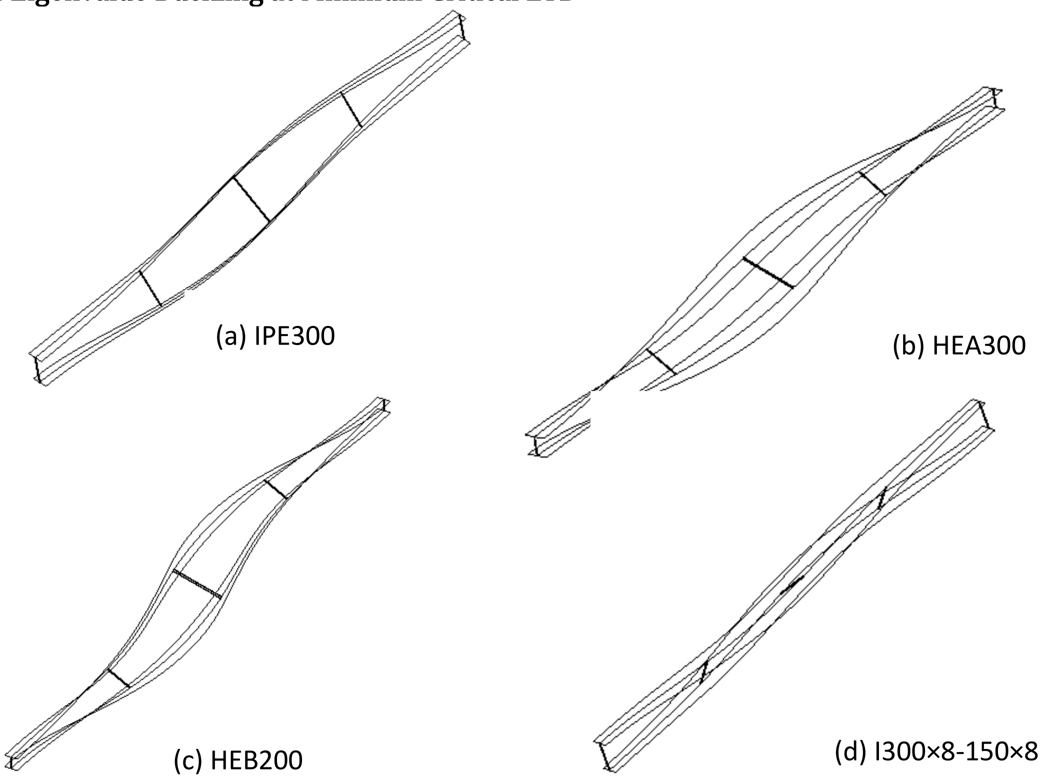

Fig. 15: Eigenvalue Buckling at Minimum Critical LTB (Case D)

3.4 Justification

By observing the recurring patterns of this phenomenon, it was found that there must be two conditions for its occurrence.

1- The beams shall be laterally restrained at one end at least.
2- The moment diagram shall have N shape "Fig. 16" through points:M_1, M_2, M_3, M_4 such that:
- $M_1 \approx M_3$
- $M_2 \approx M_4$

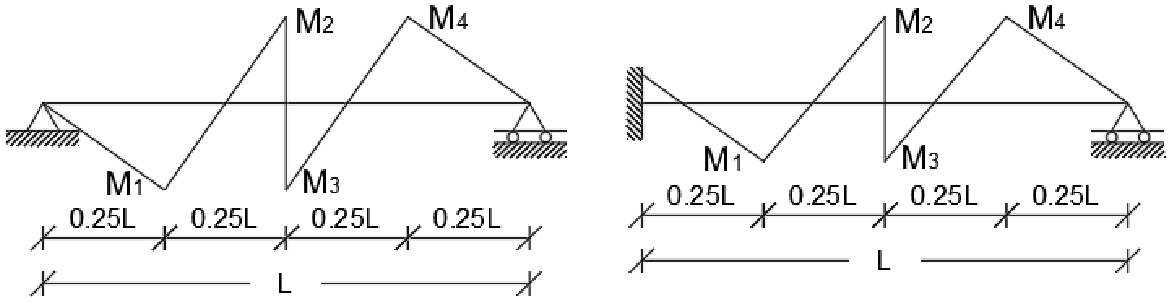

Fig. 16: Moment Gradient when $M_{cr} < M_{Fundamental}$

The recurring of this phenomenon with changing the location and tightness of the N shape needs to be studied in future research. Regardless, it was believed that the moment gradient formulas need to be developed due to the possibility that for some moment diagrams or boundary conditions, the equations give incorrect results [12] [11] [5], However, the paper shows it is required to develop the moment gradient formulas because they could also be less than one.

4. Conclusion.

The elastic critical moment is an important aspect of lateral-torsional buckling design. Standards, spreadsheets, and structural analysis programs use the moment gradient factor or equivalent moment factor to relate the critical LTB from different moment diagrams to the fundamental M_{cr}. It was thought that the fundamental critical moment is the most critical case. Almost no research can be found for loading cases where the critical LTB is less than the fundamental M_{cr} due to variation in the bending diagram and lateral boundary conditions, thus causing the moment factor to be less than one.
The study discovers a new phenomenon where the actual critical moment is less than the fundamental critical moment. This phenomenon was achieved in loading cases consisting of an intermediate moment and two inverted forces, which are tracked throughout the variation of loading ratios and locations.
Accordingly, the study provides the following recommendations and suggestions for future researches:

1- It is required to recognize that the actual critical LTB could be less than the fundamental critical moment, and it is essential to realize that taking the moment gradient factor equal to 1 is not always conservative. In other words, the moment gradient factor, Cb = 1 overestimate the LTB buckling strength for cases studied herein.
2- This phenomenon occurs under two conditions; First, when the beam is laterally restrained at ends. Second, when the moment gradient is similar to N shape,
3- It is recommended to study the actual critical buckling moment for singly-symmetric I-shapes under the presented loading conditions since it is equal to the fundamental (LTB) for T-shaped beams susceptible to elastic lateral–torsional buckling in the CSA S16 and AISC 360,
4- It is required to investigate the critical buckling moment on channels and cold-formed sections subjected to the same loading scenarios since it could be less than the fundamental (LTB) shown in I sections here.
5- It is recommended to improve the moment gradient expressions included within the standards and exclude formulas that give results not less than one,

5. Data Availability Statement:

All data, models, or code that support the findings of this study are available from the corresponding author upon reasonable request.

References

[1] T. Ncci, "NCCI : Elastic critical moment for lateral torsional buckling," pp. 1–13.
[2] S. Timoshenko and J.M. Gere, "Theory of elastic stability." McGRAW-HILL, 1961.

[3] N. S. Trahair, *Flexural-torsional buckling of structures*. CRC, 1993.

[4] C. H. Yoo and S. C. Lee, “Torsional and Flexural-Torsional Buckling,” in *Stability of Structures*, Elsevier, 2011, pp. 303–326.

[5] B. Suryoatmono and D. Ho, “The moment-gradient factor in lateral-torsional buckling on wide flange steel sections,” 2002. [Online]. Available: www.elsevier.com/locate/jcsr.

[6] C. Carter, T. Murray, and W. Thornton, “Economy in steel,” *Mod. Steel Constr.*, 2000.

[7] AISC, “AISC 360-16: Specification for Structural Steel Buildings,” *Am. Inst. Steel Constr.*, 2016.

[8] “EN 1993-1-1 (2005),” vol. 1, no. 2005, 2011.

[9] “Rules-for-Member-Stability-in-en-1993-1-1.pdf.” .

[10] K. Wierzbicki, “Influence of Warping on Bearing Capacity of Steel I-Beam with Non-Fork Support,” in *IOP Conference Series: Materials Science and Engineering*, Feb. 2019, vol. 471, no. 5, doi: 10.1088/1757-899X/471/5/052023.

[11] M. A. Serna, L. Aitziber, and D. J. Yong, “Equivalent uniform moment factors for lateral – torsional buckling of steel members,” vol. 62, pp. 566–580, 2006, doi: 10.1016/j.jcsr.2005.09.001.

[12] A. López, D. J. Yong, and M. A. Serna, “STABILITY AND DUCTILITY OF STEEL STRUCTURES LATERAL-TORSIONAL BUCKLING OF STEEL BEAMS : A GENERAL EXPRESSION FOR THE MOMENT GRADIENT FACTOR,” 2006.

[13] J. Westlund, “Lateral Torsional Buckling of I-beams,” 2013.

[14] “Bathe, K.-J. - Finite Element Procedures - 1996 - Prentice-Hall - ISBN 0133014584 - 1052s.”

[15] L. Subramanian, W. Y. Jeong, R. Yellepeddi, and D. W. White, “Assessment of I-Section Member LTB Resistances Considering Experimental Test Data and Practical Inelastic Buckling Design Calculations,” *Eng. Journal-American Inst. Steel Constr.*, vol. 55, no. 1, pp. 15–44, 2018.

[16] M. Secer and E. Turker Uzun, “Elastic Lateral Torsional Buckling of Simply Supported Beams under Concentrated Load and Linear Moment Gradient,” in *IOP Conference Series: Materials Science and Engineering*, Nov. 2017, vol. 245, no. 3, doi: 10.1088/1757-899X/245/3/032077.

[17] CTICM, “LTBeam – Report on Validation Tests,” no. July, pp. 1–21, 2002.

[18] H. J. W. Smalberger, “Comparative study of the equivalent moment factor between international steel design specifications,” no. December, 2014.

[19] E. Wong and R. G. Driver, “Critical evaluation of equivalent moment factor procedures for laterally unsupported beams,” *Eng. J.*, vol. 47, no. 1, pp. 1–20, 2010, Accessed: Jan. 03, 2022. [Online]. Available: https://www.aisc.org/products/engineering-journal/critical-evaluation-of-equivalent-moment-factor-procedures-for-laterally-unsupported-beams/.

[20] M. Manarin, R. G. Driver, and Y. Li, “Moment Gradient Factor for Lateral-Torsional Buckling of T-Shaped Beams.”